arXiv:1604.08945v1 [cond-mat.mtrl-sci] 29 Apr 2016

Unusual electronic properties of LaBi - a new topological semimetal candidate

Yun Wu,[1,2] Tai Kong,[1,2] Lin-Lin Wang,[1] D. D. Johnson,[1,2,3]
Daixiang Mou,[1,2] Lunan Huang,[1,2] Benjamin Schrunk,[1,2]
S. L. Bud'ko,[1,2] P. C. Canfield,[1,2,*] and Adam Kaminski[1,2,†]

[1]*Division of Materials Science and Engineering, Ames Laboratory, Ames, Iowa 50011, USA*

[2]*Department of Physics and Astronomy, Iowa State University, Ames, Iowa 50011, USA*

[3]*Department of Materials Science and Engineering, Iowa State University, Ames, Iowa 50011, USA*

(Dated: May 28, 2022)

Abstract

We use density functional theory calculations and ARPES measurements to study the electronic properties of LaBi, a binary system that was proposed to be a member of a new family of topological semimetals. Both bulk and surface bands are present in the spectra. The dispersion of the surface state is highly unusual. It resembles a Dirac cone, but upon closer inspection we can clearly detect an energy gap. The bottom band follows roughly a parabolic dispersion. The top band has an unusual linear "V" shape dispersion with the tip approaching very closely to the bottom band. Our data suggests that this compound hosts unusual, yet to be understood topological state.

The discovery of Quantum Hall Effect[1] has introduced quantum states that can not be classified by spontaneous symmetry breaking, instead they are classified by their topology. Another topological state, Quantum Spin Hall state, has been theoretically predicted and experimentally observed in HgTe quantum wells[2,3]. This new topological state exists in a system that is insulating in its bulk but topologically conducting on the edge (i. e. 1D equivalent of 2D surface). BiSb binary was the first bulk material verified to be a topological insulator by use of angle-resolved photoemission spectroscopy (ARPES) that directly probes the electronic structure[4,5]. However, its complicated surface states, fairly small bulk band gap and alloying disorder made it hard to be a model system for studying topological quantum phenomena and technological applications. Bi_2Se_3, Bi_2Te_3 and Sb_2Te_3 were theoretically predicted[6] and experimentally proved to be the second generation topological insulators with a single Dirac cone residing at the Γ point[7,8]. The surface Dirac cone states are protected by time reversal symmetry (TRS). Therefore, TRS breaking sources, such as magnetic field or magnetic dopant can modify the massless electrons into massive electrons[9].

Discovery of such topologically protected quantum state generated a lot of interest and sparked search for novel, exotic topological states, such as three-dimensional Dirac semimetals[10–15], type-I and type-II Weyl semimetals[16–31] and line node semimetals[32–34]. However, no new family of binary topological insulators was reported to date. Recently, simple rock salt rare earth monopnictides LaX (X = N, P, As, Sb, Bi) were predicted to host novel topological states, such as "linked nodal ring" in LaN when spin-orbital coupling is neglected[35]. When considering the spin-orbital coupling, LaN turns into a three-dimensional Dirac semimetal and the rest of the family turn into topological insulators[35]. Here, we present the results from our laser-based ARPES measurements and density functional theory (DFT) calculations detailing the electronic structure of LaBi. The dispersion of the surface state is highly unusual. It resembles a Dirac cone, but upon closer inspection we can clearly detect an energy gap. The bottom band follows roughly a parabolic dispersion. The top band has an unusual linear "V" shape dispersion with the tip approaching very closely to the bottom band. Our data suggests that this compound hosts unusual, yet to be understood topological state.

Single crystals of LaBi were grown using a high-temperature solution growth technique[36]. Starting elements (La from Ames Laboratory and Bi from Alfa Aesar, 99.99% purity) were packed in a frit-disc alumina crucible set[37] with a molar ratio of La: Bi = 30: 70. The

crucible with the starting materials were sealed in a silica ampoule under a partial argon atmosphere. The whole ampoule was then heated up to 1200 °C, held at 1200 °C for 3 hours and slowly cooled to 1000 °C, at which temperature the solution and the single crystals were quickly separated in a centrifuge. Single crystals of LaBi are cubic in shape with a typical edge length of 0.5 mm. ARPES measurements were carried out using a laboratory-based system consisting of a Scienta R8000 electron analyzer and a a tunable VUV laser light source[38]. The data were acquired using a tunable VUV laser ARPES system, consisting of a Scienta R8000 electron analyzer, picosecond Ti:Sapphire oscillator and fourth harmonic generator. Data were collected with a tunable photon energy from 5.64 eV to 6.70 eV. Angular resolution was set at $\sim 0.05^\circ$ and 0.5° (0.005 Å^{-1} and 0.05 Å^{-1}) along and perpendicular to the direction of the analyzer slit (and thus cut in the momentum space), respectively; and energy resolution was set at 1 meV. The size of the photon beam on the sample was $\sim$30 μm. Samples were cleaved *in situ* at a base pressure lower than 1×10^{-10} Torr. Samples were cooled using a closed cycle He-refrigerator and the sample temperature was measured using a silicon-diode sensor mounted on the sample holder. The energy corresponding to the chemical potential was determined from the Fermi edge of a polycrystalline Au reference in electrical contact with the sample. Samples were cleave at 40K and were kept at the cleaving temperature throughout the measurement. Density functional theory[39,40] (DFT) calculations have been done in VASP[41,42] using PBE[43] exchange-correlation functional, plane-wave basis set with projected augmented waves[44] and spin-orbital coupling (SOC) effect included. For bulk band structure of LaBi, we use the conventional orthorhombic cell of 20 atoms with a Monkhorst-Pack[45] $(8 \times 6 \times 8)$ k-point mesh. For surface band structure, we use slabs up to 96 atomic layers or 320 atoms with a $(8 \times 1 \times 8)$ k-point mesh and at least a 12 Å vacuum. The kinetic energy cutoff is 230 eV. The convergence with respect to k-point mesh was carefully checked, with total energy converged, e.g., well below 1 meV/atom.

The crystal structure, Fermi Surface (FS) and band dispersion along key directions in the Brillouin Zone (BZ) for LaBi are shown in Fig.1. Panel (b) shows the ARPES intensity measured at the chemical potential using He-I line (21.2 eV) at $T = 37$ K. The data was integrated within 10 meV to improve statistics. High intensity areas mark the contours of the FS sheets. The FS consists of electron and hole pockets at the Γ point and two elliptical electron pockets at the M point (black dashed lines are guide to the eye). The FS resembles

the calculated bulk-band FS from DFT as shown in Fig.1c. Panels (d)–(f) show the band dispersion measured using ARPES along cuts no.1–no.3 in Fig.1b. Panels (g)–(i) show the corresponding surface band calculations with 48-layer slab along those same cuts shown in panel (d)–(f). Panel (j) shows the bulk band calculation. In panel (d), we can see two electron pockets with the smaller one being enclosed by the bigger one, which agrees with the surface and bulk-band calculation results shown in panel (g) and (j). Panel (e) shows the band dispersion along the cut no.2 at the crossing point of the $d-p$ orbital mixing. This feature looks very much like a Dirac cone, except that the calculation shows a possible gap separating the top and bottom bands.. Our DFT calculations results are similar with the results in Ref.[35] in which topological surface state was predicted to reside in the $d-p$ band inversion regime. However, due to limited resolution and limited tunability of the photon energy in the He-lamp ARPES system, we cannot verified its surface origin by probing its out of plane momentum dispersion. At the Γ point (panel (f)), an electron pocket is clearly seen. However, no details can be resolved at higher binding energies. Panel (i) show the calculated surface-band dispersion along the same cut in panel (f), which resembles main features measured by ARPES results. As it is shown in panel (i), the Dirac surface state (if it exists) is buried deep in the bulk state at the Γ point (consistent with the conclusion in Ref.[35]) that this topological state may not be observed in (001) surface projection.

To reveal the details of these states we used tunable vacuum ultraviolet laser ARPES spectrometer. The ability to tune photon energy combined with small beam spot and ultrahigh resolution allows us to gain more information about these features. Figure 2 shows the constant energy contours and data along high symmetry cut along with results of DFT surface-band calculations using a slab method. Panel a shows the constant energy contours measured at 40 K and photon energy of 6.7 eV. The constant energy contour at the Fermi level shows an isotoxal square star shape with a circle that can be vaguely seen at the center. At the binding energy of 200 meV, a circular energy contour can be clearly observed, surrounded by square shape bulk band intensities. Further moving down to 280 meV below the Fermi level, a single dot, i.e., the Dirac-like point can be easily distinguished from the bulk band contributions. At binding energy of 400 meV, a single perfect circular energy contour emerges, i.e., cross section of the lower half of what would be a surface Dirac cone. Panel b shows the constant energy contours from DFT calculations with 16-layer slab, which also shows the evolution of the Dirac cone-like feature from a circular contour to a single

Dirac point and further to a circular contour, which may not be easily resolved because of all the bulk band projection. The surface Dirac cone-like can be better visualized in the high symmetry cut (panel c) along cut no.1 in Fig.2. The bulk conduction band crosses the Fermi level and the top of the bulk valence band is visible in panel c. The conduction and valence band appear to be connected by the topological surface state. Panel d shows the calculated surface state with 48-layer slab, which demonstrates that the surface state is buried in the bulk state projection. This is consistent with the data shown in panel a and it is also consistent with previously reported results[35].

We utilize photon energy dependent ARPES data (with rather fine energy steps 0.13 eV) to distinguish between bulk and surface states. The detailed results measured using photon energies from 6.7 eV to 5.64 eV are presented in Fig.3. A single Dirac-like dispersion is present across higher photon energies (top row of data in panel (a)) with no obvious change in shape. However, the size of the conduction electron pocket and intensity of bulk hole band changes drastically especially for lower photon energies. In order to qualitatively determine the change in the size of the conduction electron pocket, we have plotted the momentum dispersion curves at the Fermi level in panel (b), which clearly shows an increase of the electron pocket size with decreasing incident photon energies. For the four highest photon energy we plot the MDC's at binding energies of 200 meV (top part of Dirac cone-like feature) and 320 meV (bottom part of Dirac cone-like feature). Constant separation between the MDC peaks demonstrates surface origin or quasi two dimensionality of this feature.

The key question here is whether or not this is exactly a Dirac dispersion with no energy gap and apparent degeneracy of electronic states at the Dirac point. To examine this we use EDC's and look for the presence of an energy gap. The band dispersion along Γ cut measured with 6.7 eV photons is shown in Fig. 4(a) and set of EDC's equally spaced in the momentum is shown in Fig. 4(c). The EDC at the suspected location of Dirac point shows a peak that originates from bottom part of the dispersion and a distinct shoulder at lower binding energy that originates from the upper band. The two peaks fits to EDC at the Γ are shown in Fig. 4d. This signifies presence of an energy gap separating the two bands and it demonstrates that prominent Dirac-like feature is not a "traditional" Dirac cone. However, this is not a trivial band dispersion either. While the bottom part of the band is parabolic, the top part is highly linear with pronounced cusp pointing towards the bottom band. This can be seen better in dispersion fits to EDC and MDC data shown in

Fig. 4(b). While EDC analysis seems to imply presence of an energy gap separating the top and bottom parts, We cannot exclude a possibility of the two portions being merged at a point and the being an artifact due to combination of experimental resolution and very low density of states at the tip of the cusp. In summary, we studied the electronic properties of newly proposed topological semimetal LaBi. The dispersion of the surface state is highly unusual. It resembles a Dirac cone, but upon closer inspection we can possibly detect an energy gap. The bottom band follows roughly a parabolic dispersion. The top band has an unusual linear "V" shape dispersion with the tip approaching very closely to the bottom band. Our data suggests that this compound likely hosts unusual, yet to be understood topological state.

ACKNOWLEDGEMENTS

This work was supported by the U.S. Department of Energy, Office of Science, Basic Energy Sciences, Materials Science and Engineering Division. Ames Laboratory is operated for the U.S. Department of Energy by Iowa State University under contract No. DE-AC02-07CH11358. L. H. was supported by CEM, an NSF MRSEC, under grant DMR-1420451.

CORRESPONDING AUTHOR

Correspondence to: Adam Kaminski, email: kaminski@ameslab.gov; Paul C. Canfield, email: canfield@ameslab.gov.

REFERENCES

---

* canfield@ameslab.gov

† kaminski@ameslab.gov

[1] K. v. Klitzing, G. Dorda, and M. Pepper, Phys. Rev. Lett. **45**, 494 (1980).

[2] B. A. Bernevig, T. L. Hughes, and S.-C. Zhang, Science **314**, 1757 (2006).

[3] M. König, S. Wiedmann, C. Brüne, A. Roth, H. Buhmann, L. W. Molenkamp, X.-L. Qi, and S.-C. Zhang, Science **318**, 766 (2007).

[4] L. Fu and C. L. Kane, Phys. Rev. B **76**, 045302 (2007).

[5] D. Hsieh, D. Qian, L. Wray, Y. Xia, Y. S. Hor, R. J. Cava, and M. Z. Hasan, Nature **452**, 970 (2008).

[6] H. Zhang, C.-X. Liu, X.-L. Qi, X. Dai, Z. Fang, and S.-C. Zhang, Nat. Phys. **5**, 438 (2009).

[7] Y. Xia, D. Qian, D. Hsieh, L. Wray, A. Pal, H. Lin, A. Bansil, D. Grauer, Y. S. Hor, R. J. Cava, and M. Z. Hasan, Nat. Phys. **5**, 398 (2009).

[8] Y. L. Chen, J. G. Analytis, J.-H. Chu, Z. K. Liu, S.-K. Mo, X. L. Qi, H. J. Zhang, D. H. Lu, X. Dai, Z. Fang, S. C. Zhang, I. R. Fisher, Z. Hussain, and Z.-X. Shen, Science **325**, 178 (2009).

[9] Y. L. Chen, J.-H. Chu, J. G. Analytis, Z. K. Liu, K. Igarashi, H.-H. Kuo, X. L. Qi, S. K. Mo, R. G. Moore, D. H. Lu, M. Hashimoto, T. Sasagawa, S. C. Zhang, I. R. Fisher, Z. Hussain, and Z. X. Shen, Science **329**, 659 (2010).

[10] Z. Wang, Y. Sun, X.-Q. Chen, C. Franchini, G. Xu, H. Weng, X. Dai, and Z. Fang, Phys. Rev. B **85**, 195320 (2012).

[11] Z. K. Liu, B. Zhou, Y. Zhang, Z. J. Wang, H. M. Weng, D. Prabhakaran, S.-K. Mo, Z. X. Shen, Z. Fang, X. Dai, Z. Hussain, and Y. L. Chen, Science **343**, 864 (2014).

[12] Z. Wang, H. Weng, Q. Wu, X. Dai, and Z. Fang, Phys. Rev. B **88**, 125427 (2013).

[13] M. Neupane, S. Xu, R. Sankar, N. Alidoust, G. Bian, C. Liu, I. Belopolski, T. Chang, H. Jeng, H. Lin, A. Bansil, F. Chou, and M. Z. Hasan, Nat Commun **5** (2014).

[14] Z. K. Liu, J. Jiang, B. Zhou, Z. J. Wang, Y. Zhang, H. M. Weng, D. Prabhakaran, S.-K. Mo, H. Peng, P. Dudin, T. Kim, M. Hoesch, Z. Fang, X. Dai, Z. X. Shen, D. L. Feng, Z. Hussain, and Y. L. Chen, Nat Mater **13**, 677 (2014).

[15] A. Narayanan, M. D. Watson, S. F. Blake, N. Bruyant, L. Drigo, Y. L. Chen, D. Prabhakaran, B. Yan, C. Felser, T. Kong, P. C. Canfield, and A. I. Coldea, Phys. Rev. Lett. **114**, 117201 (2015).

[16] S. Huang, S. Xu, I. Belopolski, C. Lee, G. Chang, B. Wang, N. Alidoust, G. Bian, M. Neupane, C. Zhang, S. Jia, A. Bansil, H. Lin, and M. Z. Hasan, Nat Commun **6** (2015).

[17] H. Weng, C. Fang, Z. Fang, B. A. Bernevig, and X. Dai, Phys. Rev. X **5**, 011029 (2015).

[18] S.-Y. Xu, I. Belopolski, N. Alidoust, M. Neupane, G. Bian, C. Zhang, R. Sankar, G. Chang, Z. Yuan, C.-C. Lee, S.-M. Huang, H. Zheng, J. Ma, D. S. Sanchez, B. Wang, A. Bansil, F. Chou,

P. P. Shibayev, H. Lin, S. Jia, and M. Z. Hasan, Science **349**, 613 (2015).

[19] S. Xu, N. Alidoust, I. Belopolski, Z. Yuan, G. Bian, T. Chang, H. Zheng, V. N. Strocov, D. S. Sanchez, G. Chang, C. Zhang, D. Mou, Y. Wu, L. Huang, C. Lee, S. Huang, B. Wang, A. Bansil, H. Jeng, T. Neupert, A. Kaminski, H. Lin, S. Jia, and M. Zahid Hasan, Nat Phys **11**, 748 (2015).

[20] S.-Y. Xu, I. Belopolski, D. S. Sanchez, C. Zhang, G. Chang, C. Guo, G. Bian, Z. Yuan, H. Lu, T.-R. Chang, P. P. Shibayev, M. L. Prokopovych, N. Alidoust, H. Zheng, C.-C. Lee, S.-M. Huang, R. Sankar, F. Chou, C.-H. Hsu, H.-T. Jeng, A. Bansil, T. Neupert, V. N. Strocov, H. Lin, S. Jia, and M. Z. Hasan, Science Advances **1** (2015), 10.1126/sciadv.1501092.

[21] A. A. Soluyanov, D. Gresch, Z. Wang, Q. Wu, M. Troyer, X. Dai, and B. A. Bernevig, Nature **527**, 495 (2015), arXiv:1507.01603.

[22] Y. Sun, S.-C. Wu, M. N. Ali, C. Felser, and B. Yan, arXiv preprint arXiv:1508.03501 (2015).

[23] T.-R. Chang, S.-Y. Xu, G. Chang, C.-C. Lee, S.-M. Huang, B. Wang, G. Bian, H. Zheng, D. S. Sanchez, I. Belopolski, N. Alidoust, M. Neupane, A. Bansil, H.-T. Jeng, H. Lin, and M. Zahid Hasan, Nat Commun **7** (2016).

[24] I. Belopolski, S.-Y. Xu, Y. Ishida, X. Pan, P. Yu, D. S. Sanchez, M. Neupane, N. Alidoust, G. Chang, T.-R. Chang, *et al.*, arXiv preprint arXiv:1512.09099 (2015).

[25] L. Huang, T. M. McCormick, M. Ochi, Z. Zhao, M.-t. Suzuki, R. Arita, Y. Wu, D. Mou, H. Cao, J. Yan, *et al.*, arXiv preprint arXiv:1603.06482 (2016).

[26] F. Y. Bruno, A. Tamai, Q. S. Wu, I. Cucchi, C. Barreteau, A. de la Torre, S. M. Walker, S. Riccò, Z. Wang, T. K. Kim, M. Hoesch, M. Shi, N. C. Plumb, E. Giannini, A. A. Soluyanov, and F. Baumberger, arXiv (2016), arXiv:1604.02411.

[27] C. Wang, Y. Zhang, J. Huang, S. Nie, G. Liu, A. Liang, Y. Zhang, B. Shen, J. Liu, C. Hu, Y. Ding, D. Liu, Y. Hu, S. He, L. Zhao, L. Yu, J. Hu, J. Wei, Z. Mao, Y. Shi, X. Jia, F. Zhang, S. Zhang, F. Yang, Z. Wang, Q. Peng, H. Weng, X. Dai, Z. Fang, Z. Xu, C. Chen, and X. Zhou, , 1 (2016), arXiv:1604.04218.

[28] Y. Wu, N. H. Jo, D. Mou, L. Huang, S. Bud'ko, P. Canfield, and A. Kaminski, arXiv preprint arXiv:1604.05176 (2016).

[29] Y. Wu, N. H. Jo, M. Ochi, L. Huang, D. Mou, S. L. Bud'ko, P. C. Canfield, N. Trivedi, R. Arita, and A. Kaminski, Phys. Rev. Lett. **115**, 166602 (2015).

[30] S. Borisenko, Bulletin of the American Physical Society (2016).

[31] S.-Y. Xu, N. Alidoust, G. Chang, H. Lu, B. Singh, I. Belopolski, D. Sanchez, X. Zhang, G. Bian, H. Zheng, *et al.*, arXiv preprint arXiv:1603.07318 (2016).

[32] G. Bian, T.-R. Chang, R. Sankar, S.-Y. Xu, H. Zheng, T. Neupert, C.-K. Chiu, S.-M. Huang, G. Chang, I. Belopolski, D. S. Sanchez, M. Neupane, N. Alidoust, C. Liu, B. Wang, C.-C. Lee, H.-T. Jeng, C. Zhang, Z. Yuan, S. Jia, A. Bansil, F. Chou, H. Lin, and M. Z. Hasan, Nat Commun **7** (2016).

[33] L. M. Schoop, M. N. Ali, C. Straßer, V. Duppel, S. S. Parkin, B. V. Lotsch, and C. R. Ast, arXiv preprint arXiv:1509.00861 (2015).

[34] Y. Wu, L.-L. Wang, E. Mun, D. D. Johnson, D. Mou, L. Huang, Y. Lee, S. L. Bud/'ko, P. C. Canfield, and A. Kaminski, Nat Phys **advance online publication** (2016).

[35] M. Zeng, C. Fang, G. Chang, Y.-A. Chen, T. Hsieh, A. Bansil, H. Lin, and L. Fu, arXiv preprint arXiv:1504.03492 (2015).

[36] P. C. Canfield and Z. Fisk, Philosophical Magazine Part B **65**, 1117 (1992).

[37] P. C. Canfield, T. Kong, U. S. Kaluarachchi, and N. H. Jo, Philosophical Magazine **96**, 84 (2016).

[38] R. Jiang, D. Mou, Y. Wu, L. Huang, C. D. McMillen, J. Kolis, H. G. Giesber, J. J. Egan, and A. Kaminski, Review of Scientific Instruments **85**, 033902 (2014).

[39] P. Hohenberg and W. Kohn, Phys. Rev. **136**, B864 (1964).

[40] W. Kohn and L. J. Sham, Phys. Rev. **140**, A1133 (1965).

[41] G. Kresse and J. Furthmüller, Phys. Rev. B **54**, 11169 (1996).

[42] G. Kresse and J. Furthmller, Computational Materials Science **6**, 15 (1996).

[43] J. P. Perdew, K. Burke, and M. Ernzerhof, Phys. Rev. Lett. **77**, 3865 (1996).

[44] P. E. Blöchl, Phys. Rev. B **50**, 17953 (1994).

[45] H. J. Monkhorst and J. D. Pack, Phys. Rev. B **13**, 5188 (1976).

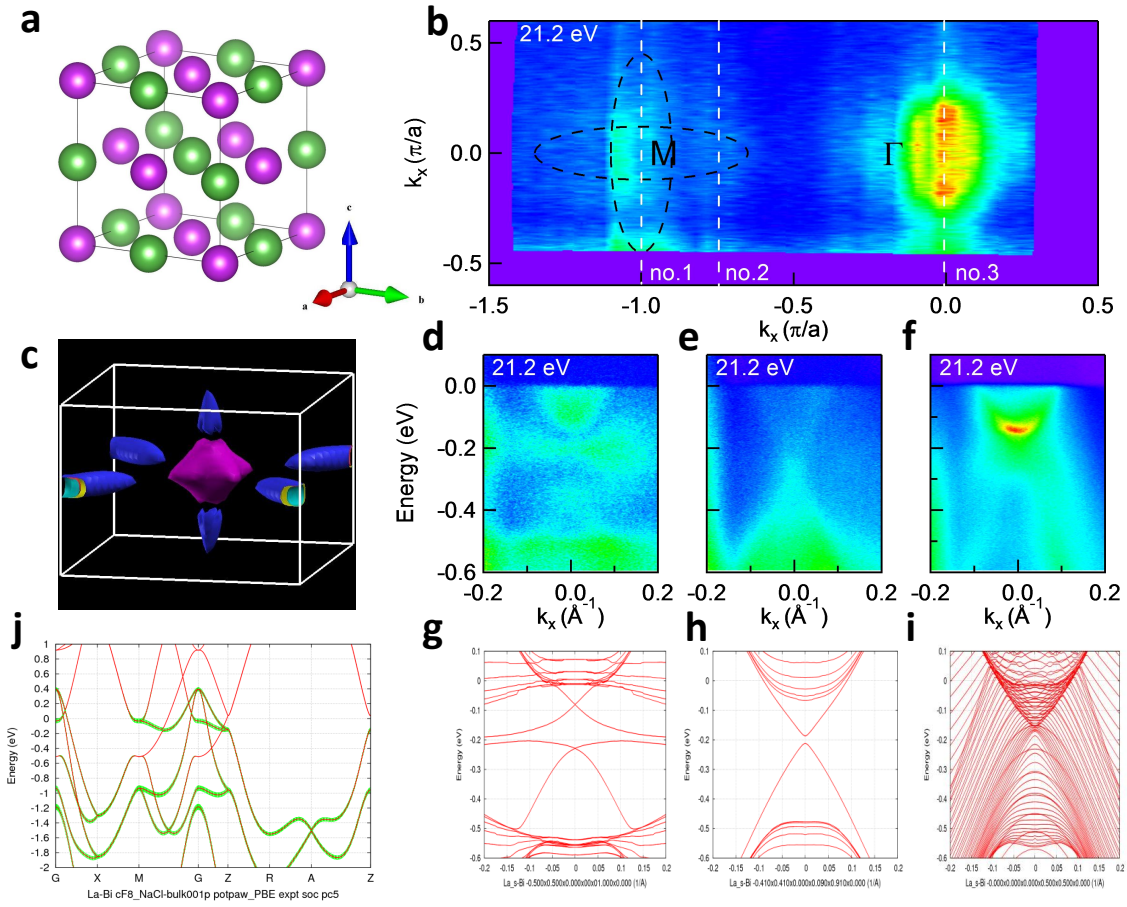

FIG. 1. (color online) Calculated and experimental Fermi surface and band dispersion of LaBi measured at T =37 K and photon energy of 21.2 eV. (a) Crystal structure (La: purple spheres, Bi: green spheres) of LaBi. (b) Fermi-surface plot of ARPES intensity integrated within 10 meV of the chemical potential along $\Gamma - M$. (c) Brillouin zone and DFT-calculated bulk FS of LaBi. (d)–(f) ARPES intensity along cuts no.1 – no.3 in (b). (g)–(i) Calculated surface-band dispersion along cuts no.1 – no.3 in (b) with 48-layer slab. (j) Calculated bulk-band dispersion along $\Gamma - M$ in (b).

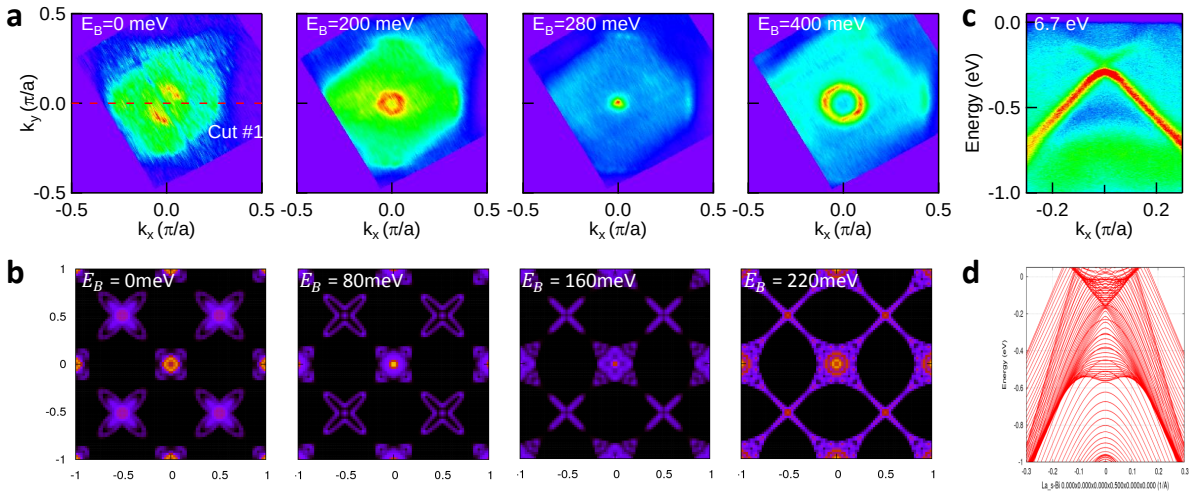

FIG. 2. (color online) Fermi surface and band dispersion in the proximity of the Γ point measured at $T = 40$ K and photon energy of 6.70 eV. (a) Constant energy contour plots of ARPES intensity integrated within 10 meV at the binding energy of 0, 200, 280 and 400 meV. (b) Constant energy contour plots of DFT surface-band calculation at the binding energy of 0, 80, 160 and 220 meV with 16-layer slab. (c) Band dispersion along cut no.1 in panel (a). (d) Calculated surface-band dispersion along $\Gamma - X$ in panel a with 48-layer slab.

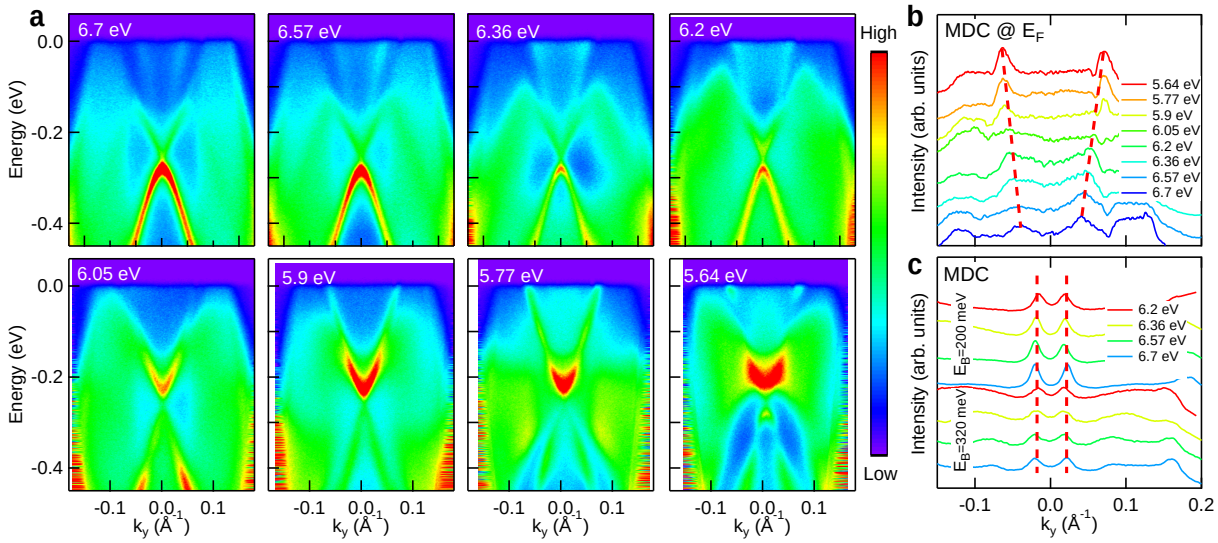

FIG. 3. (color online) Band dispersion measured at $T = 40$ K using several photon energies. (a) Band dispersion along cut no.1 in Fig.2a using photon energy of 6.70, 6.57, 6.36, 6.20, 6.05, 5.90, 5.77, and 5.64 eV. (b) Momentum dispersion curves at the chemical potential for data in panel (a). (c) Momentum dispersion curves at the binding energy of 450 meV for data in panel (a).

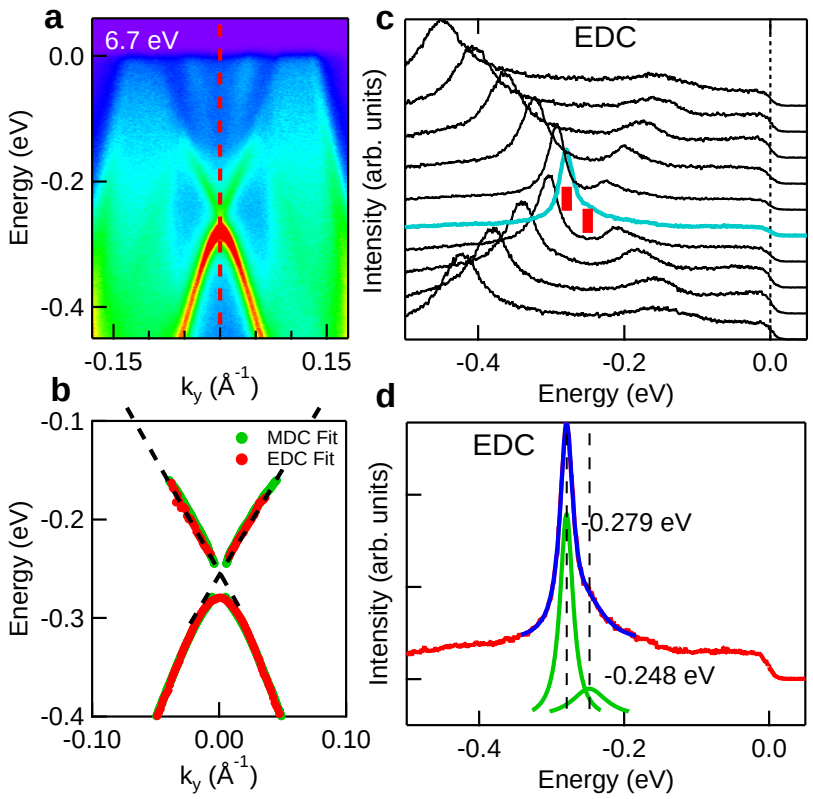

FIG. 4. (color online) (a) Band dispersion measured at along symmetry direction at Γ. (b) set of EDC's corresponding to data in (a). Red curve is measured at Γ and it reveals presence of energy gap separating upper and lower branches marked by bars. (c) Band dispersion fitted from MDC (green) and EDC (red). The black dashed lines are extension of the top Dirac like bands.